Eur. Phys. J. B **33**, 495–503 (2003)
DOI: 10.1140/epjb/e2003-00189-0

THE EUROPEAN PHYSICAL JOURNAL B

Study of the non-linear autocorrelations within the Gaussian regime

R. Kutner[a] and F. Świtała

Institute of Experimental Physics, Department of Physics, Warsaw University, Hoża, 00681 Warsaw, Poland

Received 20 March 2003
Published online 3 July 2003 –

Abstract. In this work we extend the recently considered toy model of Weierstrass or Lévy walks with varying velocity of the walker [1] by introducing a more realistic possibility that the walk can be occasionally intermitted by its momentary localization; the localizations themselves are again described by the Weierstrass or Lévy process. The direct empirical motivation for developing this combined model is, for example, the dynamics of financial high-frequency time series or hydrological and even meteorological ones where variations of the index are randomly intermitted by flat intervals of different length exhibiting no changes in the activity of the system. This combined Weierstrass walks was developed in the framework of the non-separable generalized continuous-time random walk (GCTRW) formalism developed recently [2]. This approach makes it possible to study by stochastic simulations the whole spatial-temporal range while analytically we can study only the initial, pre-asymptotic and asymptotic regions (but not the intermediate one). Our approach is possible since the Weierstrass walks is a geometric superposition of regular random walks each of which can be simply treated by stochastic simulations. This non-Markovian two-state (walking-localization) model makes possible to cover by the unified treatment a broad band of known up to now types of non-biased diffusion from the dispersive one over the normal, enhanced, ballistic, and hyperdiffusion up to the Richardson law of diffusion which defines here a part of the borderline which separates the latter from the 'Lévy ocean' where the total mean-square displacement of the walker diverges. We observed that anomalous diffusion is characterized here by three fractional exponents: temporal one characterizing the localized state and two, temporal and spatial ones, characterizing the walking state. By considering successive dynamic (even) exponents we constructed a series of different diffusion phase diagrams on the plane defined by the spatial and temporal fractional dimensions of the walking state. To adapt the model to the description of empirical data (or discrete time series) which are collected with a discrete time-step we used in the continuous-time series produced by the model a discretization procedure. We observed that such a procedure generates, in general, long-range non-linear autocorrelations even in the Gaussian regime, which appear to be similar to those observed, *e.g.*, in the financial time series [3–6], although single steps of the walker within continuous time are, by definition, uncorrelated. This suggests a surprising explanation alternative to the one proposed very recently (*cf.* [7] and Refs. therein) although both approaches involve related variants of the well-known CTRW formalism applied yet in many different branches of knowledge [8–10].

PACS. 05.45.Tp Time series analysis – 02.50.-r Probability theory, stochastic processes, and statistics – 05.40.-a Fluctuation phenomena, random processes, noise, and Brownian motion

1 Introduction

In the last few years an increased effort of statistical physicists has been observed in understanding the long-term power-law correlations present in the financial time series [11–17]. This scientific interest stems, perhaps, from the fact that (i) there is a wealth of distinctive statistical data available which suggest that the dynamics of financial markets is universal (or scale invariant); (ii) while correlations of price fluctuations decay rapidly in time, the magnitude of fluctuations (or their even non-linear function) exhibits long-term correlations. These reasons stimulated us to develop a sufficiently realistic and general toy model [2] for the analysis of empirical time-series reflecting both an active and passive behavior of a complex system in continuous time. This type of time-series consists of oblique intervals randomly intermitted by flat ones. The model belongs to the Lévy walks type characterized by finite velocity of the walker displacement and can serve as a test one for detrending fluctuation

[a] e-mail: ryszard.kutner@fuw.edu.pl

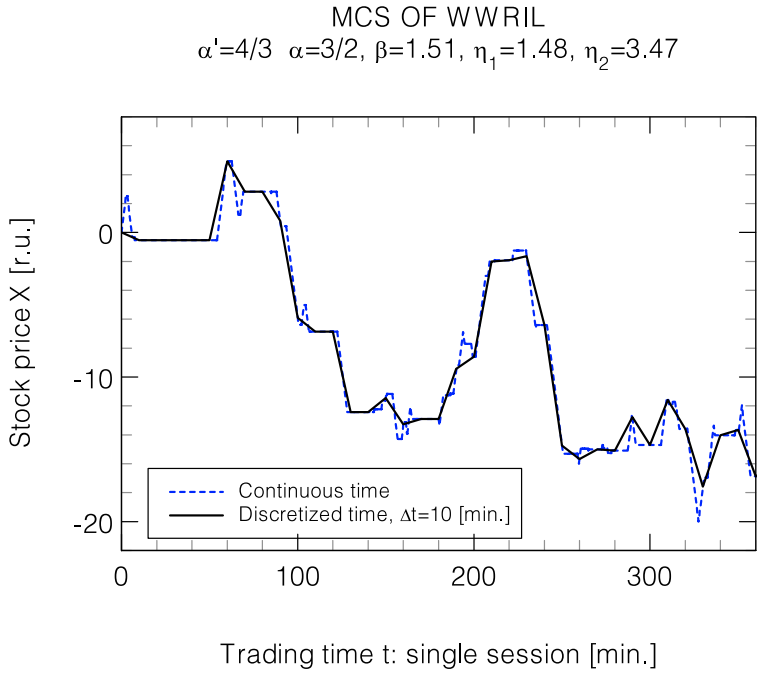

Fig. 1. Single realization (dashed curve) by the Monte Carlo simulation in continuous time of the Weierstrass random motions (oblique intervals) occasionally intermitted by localizations (flat intervals) within the non-Gaussian regime; its discretized representation for the discretization time-step $\Delta t = 10$ [min.] is given by the solid curve. Our algorithm of the Monte Carlo simulation is described in Section 4 and the applied parameters are presented in Tables 1 and 2.

analysis [18] (to verify whether trend was correctly detected and removed from the empirical data).

In this paper we used hierarchical spatial-temporal coupling (roughly justified in Sect. 2) to describe the combined physical picture exhibiting both delocalized Weierstrass random motions and localizations that are also described by the Weierstrass process. We developed a complex but more realistic version of the Weierstrass walks with varying velocity [2] namely, Weierstrass walks randomly intermitted by localizations (WWRIL). In the frame of this model the walker moves continuously at a constant velocity between the consecutive turning points where he can be occasionally and temporarily localized and then chooses direction at random, walking in principle, with an other constant velocity till the next turning point where again a localization event occurs with finite probability (*cf.* dashed curve shown in Fig. 1; we formally used the notation characteristic for financial market where the stock price is equivalent to the walker displacement). This means that at each step there is a finite probability that the walker is localized or delocalized; the walker doesn't walk all the time and his walking is randomly intermitted by periods of immobilization. When the probability of this localized state occurring vanishes this model simply tends to the Weierstrass walks with varying velocity one considered earlier [1]. Several alternative approaches were developed very recently in the context of long-term memory or autocorrelation within the CTRW formalism, *cf.* [7,19] and references therein.

As an application we use the model to create, by our Monte Carlo simulation (considered in Sect. 4), a single trajectory of the walker for any continuous time t. Next we discretize this time by using the constant discretization step Δt (which is the external parameter of the procedure) finding time moments $t_n = n\Delta t,\ n = 0, 1, \ldots$; we store the position of the walker on the trajectory only at each discrete moment t_n. We treat the set of data obtained by this procedure as our basic empirical time series (*cf.* solid curve shown in Fig. 1 where we used, for example, $\Delta t = 10$ [min.] while $\Delta t = 1$ was identified with one trading min.). In fact, we considered, within the Gaussian and non-Gaussian regimes, the high-frequency data stored at each trading minute (as by assuming longer Δt we loose too many details of the original trajectory (*cf.* again plot shown in Fig. 1). For example, in Figure 1 was present the time series obtained within the non-Gaussian regime (*cf.* the open circle (○) on the diffusion phase diagram shown in Fig. 3); the Gaussian time-series (presented, *e.g.*, by the full circle (●) on the diffusion phase diagram shown in Fig. 3) looks analogously but has, however, a geometrically narrowed vertical span. By using these time series we compared long-term autocorrelations of the absolute variations of the walker displacement present for both stochastic regimes (*cf.* Fig. 5).

Our results are particularly intriguing for the Gaussian regime where short in time correlated variations of the walker displacement (*cf.* solid curve C plotted in Fig. 4) coexist with the long-term autocorrelations of the absolute variations of the walker displacement (*cf.* solid curve K plotted in Fig. 4). This situation appears to be analogous to those often observed in different empirical time series, particularly in high-frequency financial ones [3–6].

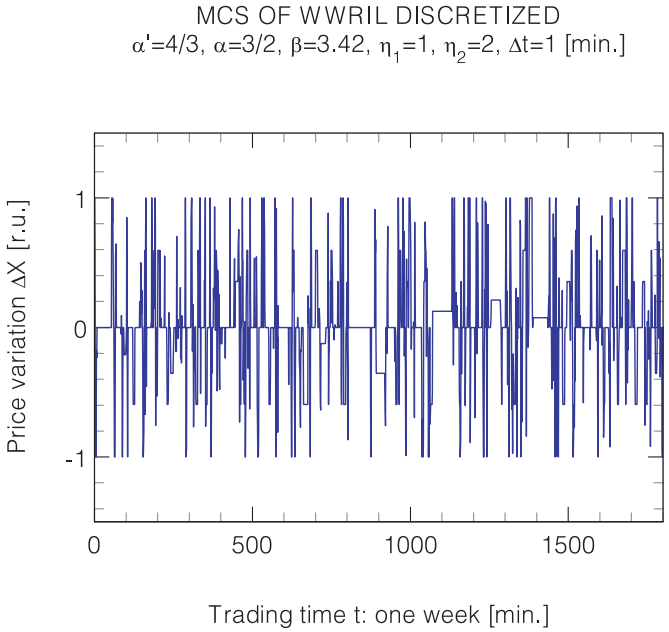

Fig. 2. The price variation, ΔX, *vs.* trading time $t_n = n\Delta t$, $n = 0, 1, \ldots$, obtained from our discretized high-frequency data stored for the Weierstrass walks randomly intermitted by temporary localizations. Several levels of the stochastic hierarchy of ΔX (located within the band of $-1 \leq \Delta X \leq 1$) are well seen, for example, for one trading week.

2 Basic definitions and quantities

In this paper we pay attention mainly to the statistics regarding single steps of the walker, *i.e.* waiting-time distributions and sojourn probabilities for walking and localization states; they constitute a foundation both for our generalized continuous-time random walk formalism (GCTRW)[1] and the Monte Carlo algorithm. Basing on the hierarchical structure of these quantities we define the effective Monte Carlo algorithm for simulation of the two-state (walking and localization) Weierstrass walks.

After discretization of time, the stochastic hierarchical structure is also well seen, for example for the dynamics of the variations of the stock price, ΔX, shown in Figure 2. However, we prove in this paper that these two descriptions of random walks (in continuous and in discrete times) are, in our case, essentially different even for asymptotic long times. The main difference arises from the fact that in the continuous time the single steps of the walker are uncorrelated (for non-vanishing time intervals) both in the linear and non-linear sense, while after discretization of time the single steps are at least non-linearly correlated. This can be understood by assuming that the discretization procedure defines a kind of random walk on a basic random walk which automatically introduces correlations even if the basic random walk were to be uncorrelated.

Walking state. In our recent series of papers [1] we considered in detail the waiting-time distribution and sojourn probability (which are the basic ones), as well as other relevant quantities for the walking state, where the walker moves with a fixed velocity between the turning points though, in general, this velocity can vary from one turning point to another. We adopt for the walking state the waiting-time distribution which exhibits spatial-temporal coupling, reflecting the hierarchical character of the fractional random walk,

$$\psi_{walk}(x,t) = \frac{1}{2}\sum_{j=0}^{\infty} w(j)[\delta(x - v_0 v^j t) + \delta(x + v_0 v^j t)] \times \frac{1}{\tau_0 \tau^j} \exp(-t/\tau_0 \tau^j), \quad (1)$$

where the weight $w(j)$ is defined as follows,

$$w(j) = (1 - \frac{1}{N})\frac{1}{N^j},\ N > 1,\ j = 0, 1, 2, \ldots, \quad (2)$$

and fulfils the normalization condition $\sum_{j=0}^{\infty} w(j) = 1$.

As it is seen, the kinematics within the walking state is defined by piece-wise constant velocity, $v_0 v^j$, and the mean time, $\tau_0 \tau^j$, needed to perform the single step (in the frame of the jth level of hierarchy); hence, the average distance which the walker is able to pass within this step is given by $b_0 b^j = v_0 \tau_0 v^j \tau^j$. We assumed that dimensionless mean-time, $\tau > 1$, and dimensionless distance, $b(= v\tau) > 1$ (where $b_0 = v_0 \tau_0$), which means that longer single steps which last (on the average) longer are less probable. These steps can be made both with (dimensionless) velocity: (i) $v < 1$ or (ii) $v > 1$ (the marginal case $v = 1$ is not discussed here). In case (i) the smaller velocity is less probable in contrast to case (ii), where less probable is the larger velocity. Of course, the walker's single-step displacement x made during the current time interval t is given by $x = v_0 v^j t$.

The reminiscence of the hierarchy of velocities, for example, for case (i) is presented in Figure 2 by using the discrete variable $\Delta X(t_{n+1})(= X(t_n + \Delta t) - X(t_n))$. As we expected, the variance ΔX is restricted in this case to the band limited by its maximal value $|\Delta X| = b_0(= 1)$ as $|\Delta X| = v_0(= 1)v^{j(=0)}(= 1)\Delta t(= 1)$, which also constitutes the zero-level of the hierarchy. Further levels of the hierarchy (contained within this band) are defined by the index $j = 1, 2, \ldots$, (note that Fig. 2 was obtained, by way of example, for dimensionless velocity v only a little smaller than the marginal value equal to 1, *i.e.* $v = b/\tau = 0.992$, where $b = 2.5$ and $\tau = 2.52$).

In this paper we focused on case (i) as it seems to be most proper from the point of view of the situation which we consider in this paper; however, both cases are again compared in Section 3.

In an analogous way we can write the expression for the sojourn probability, where only the frequency $1/\tau_0 \tau^j$

[1] The full GCTRW formalism is developed in a separate work; it is a straightforward generalization of our previous works [1] considering continuous-time Weierstrass walks with varying velocity. In the present paper we exploit only the basic elements of the GCTRW formalism necessary to consider the non-linear autocorrelations.

under the sum over j is removed in (1) (*cf.* also definitions in [1]).

Localized state. The waiting-time distribution for temporal localization of the walker can be assumed in the form analogous to (1) by putting formally the velocity $v_0 = 0$,

$$\psi_{loc}(x,t) = \delta(x)\psi_{loc}(t) \tag{3}$$

where

$$\psi_{loc}(t) = \sum_{j=0}^{\infty} w'(j)\frac{1}{\tau_0'(\tau')^j}\exp(-t/\tau_0'(\tau')^j), \tag{4}$$

while the weight $w'(j)$ is analogously defined as $w(j)$; the other parameters $N'(>1), \tau_0', \tau'(>1)$ can differ, in general, from the corresponding prototypes of the walking state. As it is seen, the moderation of the effective kinematics of the walker is also governed by the (dimensionless) mean-time τ' of the localization and the factor N'.

Analogously, we can define the sojourn probability by removing the frequency $1/\tau_0'(\tau')^j$ from under the sum over j in (4).

It should be emphasized that single steps of the walker (both walkings and localizations) occurring in the continuous time are only δ-correlated.

Combined waiting-time distribution. Our model is based on: (i) the total waiting-time distribution which is a weighted sum of the above two conditional waiting-time distributions presenting walking, $\psi_{walk}(x,t)$, and localized $\psi_{loc}(x,t)$ states

$$\psi(x,t) = p_{walk}\psi_{walk}(x,t) + p_{loc}\psi_{loc}(x,t), \tag{5}$$

as well as (ii) on the total sojourn probability, which is again an analogous weighted sum of two conditional sojourn probabilities representing the walking and localized states; the weights obey, of course, the normalization: $p_{walk} + p_{loc} = 1$. In the extreme case $p_{walk} = 1$ the present model transforms to our previous one [1]; the role of weights is considered in Section 3.

Thanks to definitions (1–5) our algorithm makes it possible to construct: (i) single stochastic trajectories of the hierarchical random walk for any continuous time and next to perform (ii) the time discretization procedure. In this paper we focus only on the non-linear long-term autocorrelations found in the discretized version of the continuous-time Weierstrass walks with varying velocity randomly intermitted by Weierstrass temporary localizations. The present work has a phenomenological and numerical character since the full version of the model, which is a straightforward extension of our previous one [1] (where no localizations are admitted), is developed elsewhere.

3 Diffusion phase diagrams

Closed analytical representations of the statistics considered in Section 2 for the asymptotic time make it possible to construct (within the GCTRW formalism) a convenient classification scheme for different types of the continuous-time Weierstrass walks with varying velocity randomly intermitted by temporary Weierstrass localizations[2]. Different diffusion phases are treated as different universality classes defined by different dynamic exponents. This means that the asymptotic time-behaviour of an even moment, $\langle X^{2m}(t)\rangle$, of the total displacement of an arbitrary order is our basic tool. It can be proved that this quantity is finite for finite time if and only if the following constraint is obeyed

$$\frac{1}{\beta} < \frac{1}{2m} + \frac{1}{\alpha}\ ,\ m = 1,2,\ldots, \tag{6}$$

and then (for $t \gg \tau_0$) this quantity assumes the form,

$$\langle X^{2m}(t)\rangle \approx (2m)!\frac{D_m}{\Gamma(1+\eta_m)}t^{\eta_m},\ m = 1,2,\ldots, \tag{7}$$

where η_m is a dynamic (fractional) exponent and D_m a fractional coefficient (expressed in [2] but doesn't appear in explicit form in the present work). Expression (7) is a generalization of analogous ones obtained earlier for the subdiffusion [20] and very recently, within an exact fractional material derivative model, for subballistic superdiffusion [28].

In Figure 3 we present the resultant diffusion phase diagram valid for arbitrary even orders ($m = 1,2,\ldots$) of displacement defined for the temporal exponent (which characterizes localization) $\alpha'(= \ln N'/\ln\tau') > 1$. Note that this particular diffusion phase diagram was given, for example, for index $m = 2$. The formulas for dynamic exponent η_m are shown in the figure in dependence on the temporal exponent $\alpha(= \ln N/\ln\tau)$ and the spatial one $\beta(= \ln N/\ln b)$. This infinite set of dynamic exponents η_m, $m = 1,2,\ldots$, defines the corresponding set of diffusion phase diagrams while the concrete dependence of η_m on α and β (and α' when $\alpha' < 1$) defines the concrete diffusion phase (*cf.* Fig. 3).

By putting $m \to \infty$ in inequality (6) and in expressions enclosed to the diffusion phase diagram shown in Figure 3, we can conclude that only for the case where $v < 1$ (which is equivalent to $\beta > \alpha$) all moments of the walker displacement are finite for finite time. Nevertheless, the propagator in this range of parameters can be, in general, non-Gaussian. The process can be classified as the Gaussian one if and only if the spatial dynamic exponent $\beta > 2$ (see Fig. 3 where index $m = 1$ should be assumed) as then the first dynamic exponent (called the diffusion one) $\eta_1 = 1.0$.

The above considerations suggest, in the context of the financial market, that the kinetics of a given asset can be classified as a burden of higher risk if its (dimensionless) velocity $v > 1$. Moreover, we can define the order of this risk as the lowest order of the moment of the total displacement which diverges for finite time.

[2] This classification is analogous to that introduced in our earlier paper [1] for the continuous-time Weierstrass walks with varying velocity.

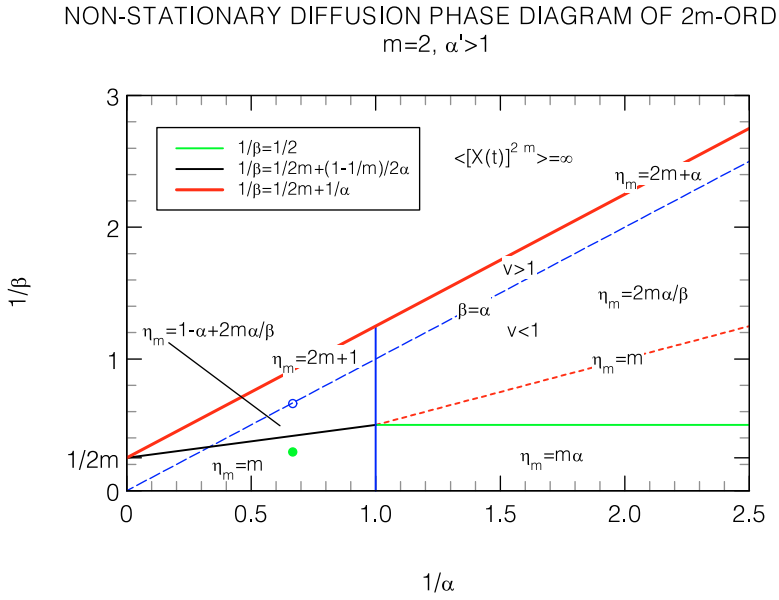

Fig. 3. Non-stationary diffusion phase diagram of $2m$-order (where $m = 1, 2, \ldots$, while here, *e.g.*, $m = 2$) for $\alpha' > 1$. The region below the bold tangent straight line relates to a finite (2m)th moment of displacement; for the remaining region this moment is infinite.

4 Hierarchical Monte Carlo simulation

This algorithm is a straightforward generalization of our previous one [1] to more realistic and more spread situations. The initial step of our efficient algorithm is the decision which states (localized or walking) should the walker occupy in the current step; this is decided simply by drawing with the proper probability p_{loc} or p_{walk}.

If we have found the state, we can perform essential next step by choosing index j with probability $p(j)$ given by

$$p(j) = \begin{cases} w(j), & \text{for walking state} \\ w'(j), & \text{for localized state.} \end{cases}$$

More precisely, we simulate a probabilistic game of random tossing of a coin. We define as a single success the situation where the coin falls to its obverse side with probability $\frac{1}{M}$, where parameter M is defined as

$$M = \begin{cases} N, & \text{for walking state} \\ N', & \text{for localized state.} \end{cases}$$

As a single defeat, occurring of course with probability $1 - \frac{1}{M}$, we define the opposite situation when the coin falls to its reverse side. We always toss our coin till the first defeat; then the number j of the successive successes is just the index we are looking for. Thus $\tau_0\tau^j$, v_0v^j and b_0b^j or $\tau'_0(\tau')^j$ are calculated (for simplicity, in all calculations we assumed $\tau_0 = 1$, $\tau'_0 = 1$, $v_0 = 1$, $b_0 = 1$). This is an efficient procedure since no drawing step is lost and always an index j is found.

In the next step of our procedure we draw from the Poisson distribution $\frac{1}{\tau^j}\exp(-\frac{\theta}{\tau^j})$ or $\frac{1}{(\tau')^j}\exp(-\frac{\theta}{(\tau')^j})$ the elapsed time interval θ of the particle remaining in the drawn state j. This time is needed for the walker to pass the distance $v_0v^j\theta$ or to remain immobile over this time interval. Note that a very long one-step walk or staying at a chosen state j could then occur.

Table 1. Exponents α', α, β, η_1 and η_2 chosen from two different places of the diffusion phase diagram.

Notation	α'	α	β	η_1	η_2
○	4/3	3/2	1.51	1.48	3.47
•	4/3	3/2	3.42	1.0	2.0

The total performance consists of several repetitions of the above two basic steps and makes it possible to simulate time series coming from both non-stationary and stationary Weierstrass or Lévy walks intermitted by temporary localizations again described by a Weierstrass or Lévy process.

For example, in Figure 1 a single realization of the Weierstrass random motions (oblique intervals) occasionally intermitted by Weierstrass localizations (flat intervals) is performed by our Monte Carlo simulation in continuous time (dashed curve); its discretized presentation (solid curve) for the discretized time-step, *e.g.* for $\Delta t = 10$ $[r.u.]$[3], is also shown (the parameters used are given in Table 1 where they are related to the open circle (○)). By assuming a much shorter discretized time-step, $\Delta t = 1$ $[r.u.]$, the discretized representation was also obtained which (unfortunately, in this resolution of the plot) cannot be distinguished from the trajectory of the corresponding continuous-time random walk process (dashed curve). The run shown in Figure 1 can be considered as

[3] Relative unit (abbreviation *r.u.*) means here the situation where $\tau_0 = \tau'_0 = 1, v_0 = 1$ and hence $b_0 = 1$.

Table 2. Microscopic parameters N', τ', N, τ and b building diffusion exponents shown in Table 1.

Notation	N'	τ'	N	τ	b
○	4	2.83	4	2.52	2.50
●	4	2.83	4	2.52	3/2

regarding a single session (or one trading day) since the data extracted from the continuous-time process running in the background have a high-frequency character (as they are recorded at every ten minute interval) and they are given only until the 360th minute.

By our algorithm we are able to simulate statistical quantities needed for analysis of the empirical time series, *e.g.*, correlation functions.

5 Algebraically decaying autocorrelations

We apply the above algorithm to calculate our basic time-dependent autocorrelation of centered absolute variations, $|\Delta X(t)| - \langle|\Delta X(t)|\rangle$, of the stock price (or the walker total displacement),

$$K(t) = \langle[|\Delta X(0)| - \langle|\Delta X(0)|\rangle][|\Delta X(t)| - \langle|\Delta X(t)|\rangle]\rangle$$
$$= \langle|\Delta X(0)||\Delta X(t)|\rangle - \langle|\Delta X(0)|\rangle\langle|\Delta X(t)|\rangle \quad (8)$$

within the Weierstrass walks randomly intermitted again by Weierstrass temporary localizations (which is, simultaneously, the autocovariance of the $|\Delta X|$ stochastic variable); here $\langle\ldots\rangle$ denotes the standard moving-average. As here, and till the end of this paper we use only discrete time we omitted index n (*cf.* Sect. 1) the more so we use the discretization step $\Delta t = 1$ [*r.u.*] which for the assumed range of time cannot allow us to distinguish between the discrete and continuous time axes in the enclosed corresponding Figures 1, 2, 4–8.

Note that our moving-average procedure was performed (in all cases) within the fixed time-window having the width of 7200 units (*e.g.* minutes when we assume $\tau_0 = \tau_0' = 1$ min; then the trading time would be four trading weeks), while the whole data block extends over 864 000 units (in the case of minutes it would be about ten trading years).

In this paper we performed, for example, calculations for two different points (marked by open (○) and full (●) circles) of the diffusion phase diagram shown in Figure 3, belonging to two different phases (the Gaussian and non-Gaussian ones, respectively). For these two points the even moment of the total displacement of arbitrary order is finite for finite time (*cf.* Sect. 3) and they are characterized by $v < 1$ which means that longer and more durable walks are slower. Hence, the single-step fractional moment of arbitrary high order is also finite for these cases.

In these two cases we have temporal exponents $1 < \alpha'$, $\alpha < 2$. Therefore, the mean times $\langle t\rangle_{walk} = (1 - 1/N)/(1 - \tau/N)$ and $\langle t\rangle_{loc} = (1 - 1/N')/(1 - \tau'/N')$ of staying in the walking and localized states, respectively, are finite (while the variances $\sigma^2_{walk}(t) = \langle t^2\rangle_{walk} - \langle t\rangle^2_{walk}$ and $\sigma^2_{loc}(t) = \langle t^2\rangle_{loc} - \langle t\rangle^2_{loc}$ diverge). Hence, in these cases the weights $p_{walk} = \langle t\rangle_{walk}/(\langle t\rangle_{walk} + \langle t\rangle_{loc})$ and $p_{loc} = \langle t\rangle_{loc}/(\langle t\rangle_{walk} + \langle t\rangle_{loc})$ are not free parameters; for these two cases they are equal and shown in Table 3.

Table 3. Weights p_{walk} and p_{loc}.

Notation	Weight p_{walk}	Weight p_{loc}
●, ○	0.44	0.56

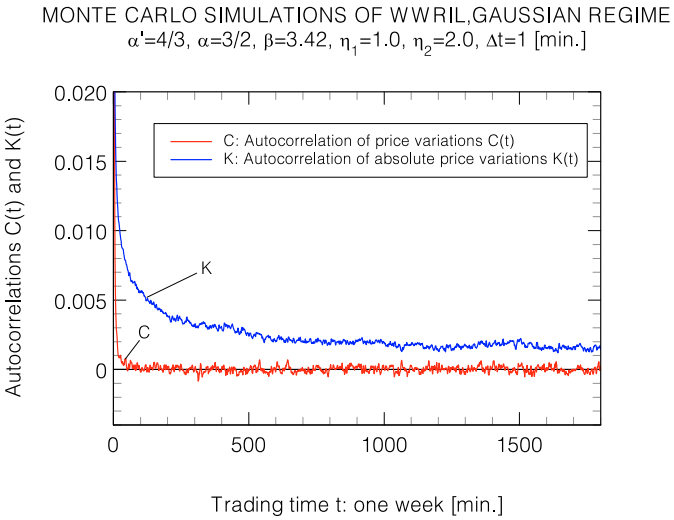

Fig. 4. Comparison between (i) autocorrelation $C(t)$ of the variations of the walker displacement (curve C), and (ii) autocorrelation $K(t)$ of the absolute variations of the walker displacement (curve K) both obtained for the Gaussian regime (represented by a full circle on diffusion phase diagram shown in Fig. 3).

In Figure 4 we compared the above defined non-linear autocorrelation function $K(t)$ with the related, linear one

$$C(t) = \langle[\Delta X(0) - \langle\Delta X(0)\rangle][\Delta X(t) - \langle\Delta X(t)\rangle]\rangle$$
$$= \langle\Delta X(0)\Delta X(t)\rangle - \langle\Delta X(0)\rangle\langle\Delta X(t)\rangle \quad (9)$$

for a chosen point denoted on the diffusion phase diagram by a full circle (●), *cf.* Figure 3, (it is, simultaneously, the autocovariance of the ΔX stochastic variable). As this point represents the Gaussian stochastic process, it gives the autocorrelation $C(t)$ plotted in Figure 4 as a quickly decaying function of time. In contrast, the plot of the non-linear autocorrelation function $K(t)$, calculated for the same process, suggests its much longer duration in time.

In Figure 5 we compare the non-linear autocorrelation function $K(t)$ for two different points, denoted on the phase diagram (plotted in Fig. 3) by the full (●) and open (○) circles, belonging to the Gaussian and non-Gaussian phases, respectively. As it is seen, in both cases the $K(t)$ obeys a power-law in time over almost three decades where the exponents for both cases are almost equal.

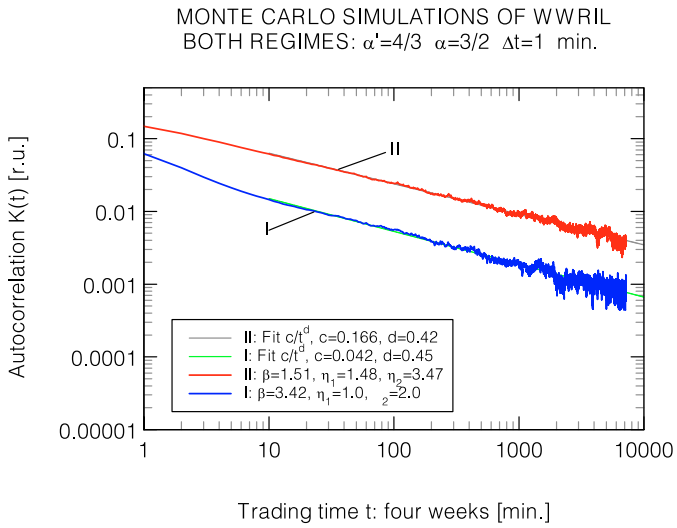

Fig. 5. Comparison between the autocorrelation functions, $K(t)$, for two different points of the diffusion phase diagram (*cf.* Fig. 3): (i) solid curve I relates to the full circle (•) belonging to the Gaussian regime, while (ii) solid curve II relates to the open circle (○) belonging to the non-Gaussian one.

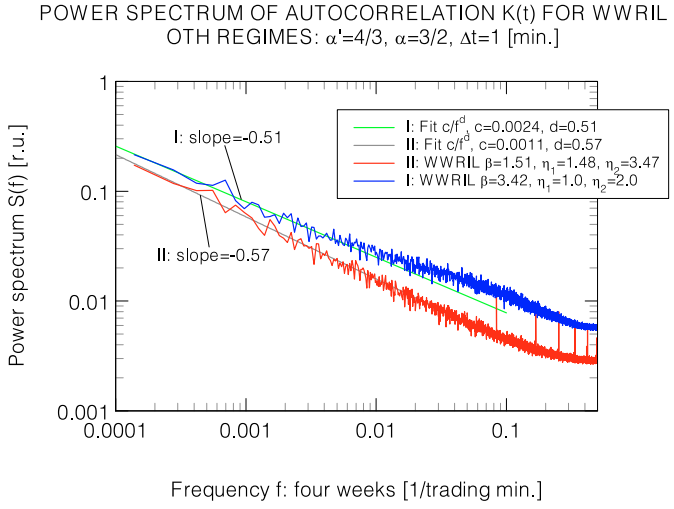

Fig. 6. Comparison between power spectra, $S(f)$, for two different points of the diffusion phase diagram (*cf.* Fig. 3): (i) solid curve I relates to the full circle (•) belonging to the Gaussian regime, while (ii) solid curve II relates to the open circle (○) belonging to the non-Gaussian one.

This result is confirmed by the dependence of the power spectrum $S(f)$ on frequency f defined as usual,

$$S(f) = \int_{-\infty}^{\infty} K(t) \exp(-\mathrm{i}2\pi f)\mathrm{d}t, \qquad (10)$$

(*cf.* Fig. 6). By comparing results shown in Figures 5 and 6 it is seen that the sum of the corresponding slopes (relating to the same points on the diffusion phase diagram shown in Fig. 3) is equal to -1 as it should be (with an error of a few percent).

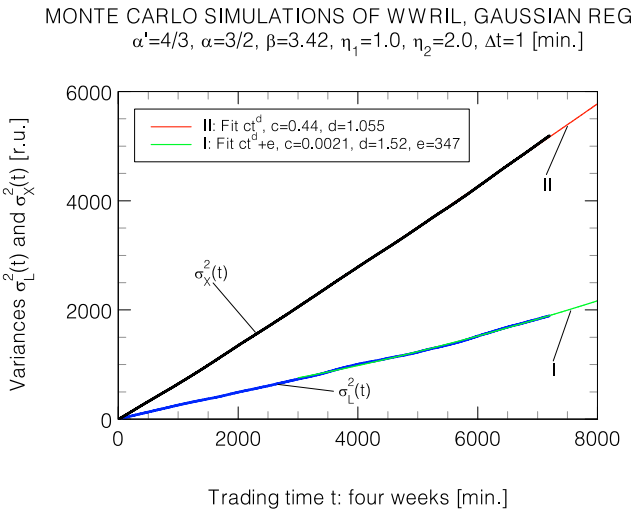

Fig. 7. The variance of the length trajectory, $\sigma_L^2(t)$, for the point of diffusion phase diagram denoted by the full circle (•) which belongs to the Gaussian regime (*cf.* Fig. 3). The superdiffusive behaviour governed by exponent 1.52 is well seen due to the corresponding fit I (shown by thin solid line partially covered by the thick one obtained by Monte Carlo simulations performed within the Weierstrass walks randomly intermitted by localizations).

In the next section we discuss the above intriguing results, however, their detailed interpretation is still an open question.

6 Discussion and concluding remarks

We found that the following two-stage procedure of extracting the non-linear long-term autocorrelations between single steps of the walker from the GCTRW, which, originally (in continuous time), doesn't exhibit this type of correlations, is necessary: (i) discretization of time (*cf.* Sect. 1), (ii) transformation from the empirical to the dual, one-sided random walk (*cf.* Fig. 8); in particular, this second stage requires explanation.

Application of the time discretization procedure with time-step Δt automatically introduces discretization of the space variable by assuming $\Delta X(t_n) = X(t_n + \Delta t) - X(t_n)$, $n = 0, 1, 2, \ldots$, as the corresponding spatial single-steps, here $X(t_n)$ and $X(t_n + \Delta t)$ are the positions of the walker on the basic (continuous-time random walk) trajectory at successive discrete time instants. This is how the empirical trajectory in Figure 8 was defined while the dual trajectory (also shown there) can develop only in the positive X-direction as it was done by transition from $\Delta X(t_n)$ (connected with the empirical trajectory) to its absolute value $|\Delta X(t_n)|$. As it is seen, this one-sided random walk obeys the feature of non-negativity of their increments; in the case of Lévy processes this relates to Lévy subordinates considered in [29].

It is the long-term autocorrelations, decaying according to the power-law, that we found to occur between the

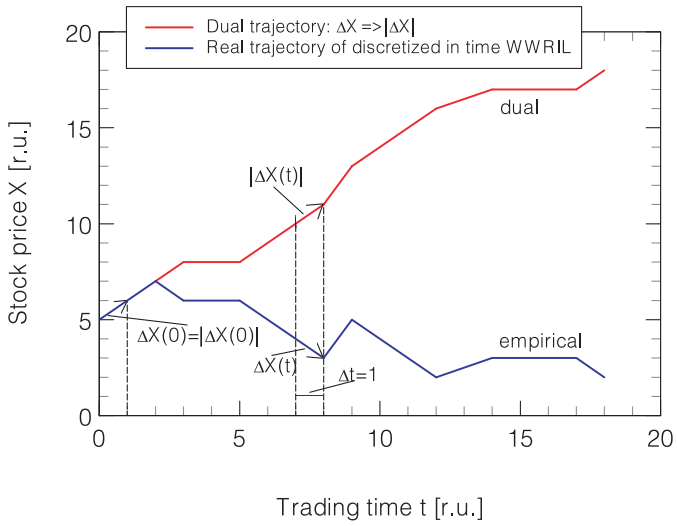

Fig. 8. Empirical and dual trajectories in discretized time where the discretization step $\Delta t = 1$ [*r.u.*]. As it is seen, the dual trajectory expands only in the positive X-direction.

single-step displacements for the dual discrete-time random walk (performed on the basic continuous-time random walk). This walk can be treated as an extreme case of directed or forward walks (with no reversals [8]) which always exhibit autocorrelations; we pointed out, to our surprise, that they are long-term ones even for the Gaussian regime which can be interpreted as a kind of 'domino effect'.

Complementarily, we consider the displacement $L(t_n)$ of the walker for the dual random walk as it is the current length of the corresponding empirical trajectory,

$$L(t_n) = \sum_{j=0}^{n-1} |\Delta X(t_j)|. \tag{11}$$

The stochastic character of the L variable arises only from the stochastic character of the velocity with which the walker covers each space interval $|\Delta X|$ within the time interval Δt. Hence, we can present the variance of the stochastic variable $L(t_n)$ in the form,

$$\begin{aligned}\sigma_L^2(t_n) &= \langle L^2(t_n)\rangle - \langle L(t_n)\rangle^2 \\ &= nK(0) + 2\sum_{j=1}^{n}(n-j)K(t_j),\end{aligned} \tag{12}$$

since the moving-average procedure doesn't distinguish a particular instant of time as the origin, leading to the stationary results. Analogously to the walker mean-square displacement (which relates to the autocorrelation C), the variance σ_L^2 is related to the autocorrelation function K. We proved that even in the Gaussian regime this quantity depends superlinearly on time for long times (*cf.* Fig. 7) which is the result of our previous observation (see Sect. 5) that the autocorrelation function $K(t)$ decays in time according to the power-law whose exponent is essentially smaller than 1 (*cf.* Fig. 4). Hence, we have two exponents bonded (with a good approximation) by its sum which equals 2, as it should be[4].

We can confirm that both the mean-square displacement and the length of the walker trajectory should be used as independent global random walk variables subject to complementary scaling relations. This was already considered, for example, in the context of random walk both on deterministic and probabilistic fractals [21–23].

Concluding we can say that in this work we developed: (a) a theoretical foundation and hence (b) an efficient algorithm which makes possible to simulate in continuous-time a quite realistic time series reflecting both the active and passive behaviour of the system for any time-horizon which exhibits scaling phenomena. The approach depends on several stochastic and kinematic parameters which can be detected by comparison with empirical data after performing a time discretization procedure. For example, (c) we applied this approach to study autocorrelations of the absolute variation of the walker single-step displacements within the Gaussian regime, which we found to decay according to the power-law in contrast to the short-time autocorrelations of the usual variation of the walker single-step displacements also present in the model. We suggest that (i) long-time autocorrelations are extorted by the discretization procedure (used to obtain data ready for comparison with the corresponding empirical ones), where the width of the time-step is (most often) incommensurable with the time interval needed to pass by the walker a single-step distance. Besides, we argue that (ii) we deal with an extreme case of forward long-time autocorrelations as no reversal walker steps are performed. In our work we presented rather observations than explanations and we suggested that the last should involved some aspects of random walk on a random walk [24–27] or more general random walk on random or disordered (*e.g.*, fractal) structures [16,21–23,26]. We suppose that our approach can be applied to study, not only financial but also other, for example, hydrological or even meteorological time-series[5].

References

1. R. Kutner, Chem. Phys. **284**, 481 (2002); R. Kutner, Comp. Phys. Comm. **147**, 565 (2002); R. Kutner, Physica A **264**, 84 (1999); R. Kutner, M. Regulski A **264**, 107 (1999)
2. R. Kutner, F. Świtała, Quantitative Finance **3**, 201 (2003); R. Kutner, F. Świtała, Lecture Notes in Comp. Science **2657**, 407 (2003)
3. P. Grau-Carles, Physica A **287**, 396 (2000)
4. H.E. Stanley, L.A.N. Amaral, X. Gabaix, P. Gopikrishnan, V. Plerou, Physica A **299**, 1 (2001)

[4] However, for superdiffusion (the non-Gaussian case) this universal number 2 is exceeded by about 10 % having, besides, a much higher prefactor.

[5] For these last two types of time-series the walker velocity can vary between successive turning points which requires further extension of our model.

5. G. Bonanno, F. Lillo, R. N. Mantegna, Physica A **299**, 16 (2001)
6. I. Giardina, J.-P. Bouchaud, Physica A **299**, 28 (2001)
7. J. Mosaliver, M. Montero, G.H. Weiss, Phys. Rev. E **67**, 021112 (2003)
8. J.W. Haus, K.W. Kehr, Phys. Rep. **158**, 263 (1987)
9. J.-P. Bouchaud, Phys. Rep. **195**, 127 (1990)
10. G.H. Weiss, *A Primar of Random Walkology, in: Fractals in Science*, edited by A. Bunde, S. Havlin (Springer-Verlag, Berlin, 1995), pp. 119–161
11. H.E. Stanley, P. Gopikrishnan, V. Plerou, L.A.N. Amaral, Quantifying fluctuations in economic systems by adapting methods of statistical physics, Physica A **287**, 339 (2000)
12. P. Gopikrishnan, V. Plerou, Y. Liu, L.A.N. Amaral, X. Gabaix, H.E.Stanley, Physica A **287**, 362 (2000)
13. V. Plerou, P. Gopikrishnan, B. Rosenow, L.A.N. Amaral, H.E. Stanley, Physica A **287**, 374 (2000)
14. P. Grau-Carles, Physica A **287**, 396 (2000)
15. Z.-F. Huang, Physica A **287**, 405 (2000)
16. J.-P. Bouchaud, Physica A **313**, 238 (2002)
17. R. Weron, Physica A **312**, 285 (2002)
18. C.-K. Peng, S.V. Buldyrev, S. Havlin, M. Simons, H.E. Stanley, A.L. Goldberger, Phys. Rev. E **49**, 1685 (1994)
19. F. Mainardi, M. Raberto, R. Gorenflo, E. Scalas, Physica A **287**, 468 (2000)
20. R. Metzler, J. Klafter, Phys. Rep. **339**, 1 (2000)
21. D. ben-Avraham, S. Mavlin, *Diffussion and Reactions in Fractals and Disordered Systems* (Cambridge University Press, Camridge, 2000); S. Havlin, Adv. Phys. **36**, 695 (1987)
22. *Fractals in Science*, edited by A. Bunde, S. Havlin (Springer-Verlag, Berlin, 1995)
23. *Fractals and Disordered Systems*, edited by A. Bunde, S. Havlin (Springer-Verlag, Berlin 1996)
24. G.H. Weiss, R.J. Rubin, J. Stat. Phys. **22**, 97 (1980)
25. K.W. Kehr, R. Kutner, Physica A **110**, 535 (1982)
26. R.C. Ball, S. Havlin, G.H. Weiss, J. Phys. A **20**, 4055 (1987)
27. R. Kutner, Physica A **171**, 43 (1991)
28. I.M. Sokolov, R. Metzler, Phys. Rev. E **67**, 010101-1-010101-4(R) (2003)
29. I. Eliazar, J. Klafter, Physica A (2003), Special Issue, *Proceedings of "Randomness and Complexity", in honor of Shlomo Havlin's 60th birthday, Eilat, January 2003* (in press)